Supporting Information

Unravelling the Spin-state of solvated $[Fe(bpp)_2]^{2+}$ Spin-crossover Complexes: Structure-Function Relationship

Maria del Carmen Giménez-López[a],* Miguel Clemente-León[b], Carlos Giménez-Saiz[b].
[a]Centro Singular de Investigación en Química Biolóxica e Materiais Moleculares (CIQUS), Universidade de Santiago de Compostela, 15782 Santiago de Compostela, Spain. E-mail: Maria.Gimenez.Lopez@usc.es
[b]Instituto de Ciencia Molecular, Universidad de Valencia, P.O. Box 22085, 46071 Valencia, Spain

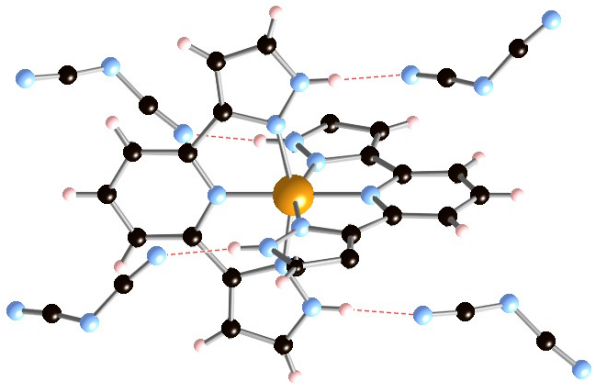

Figure S1: View of the crystal structure of the hydrated salt $[Fe(bpp)_2][N(CN)_2]_2 \cdot 1H_2O$ (**2**) showing the first and second coordination spheres for the Fe^{2+} cation. Carbon, nitrogen and hydrogen atoms are shown as black, blue and light-pink, respectively.

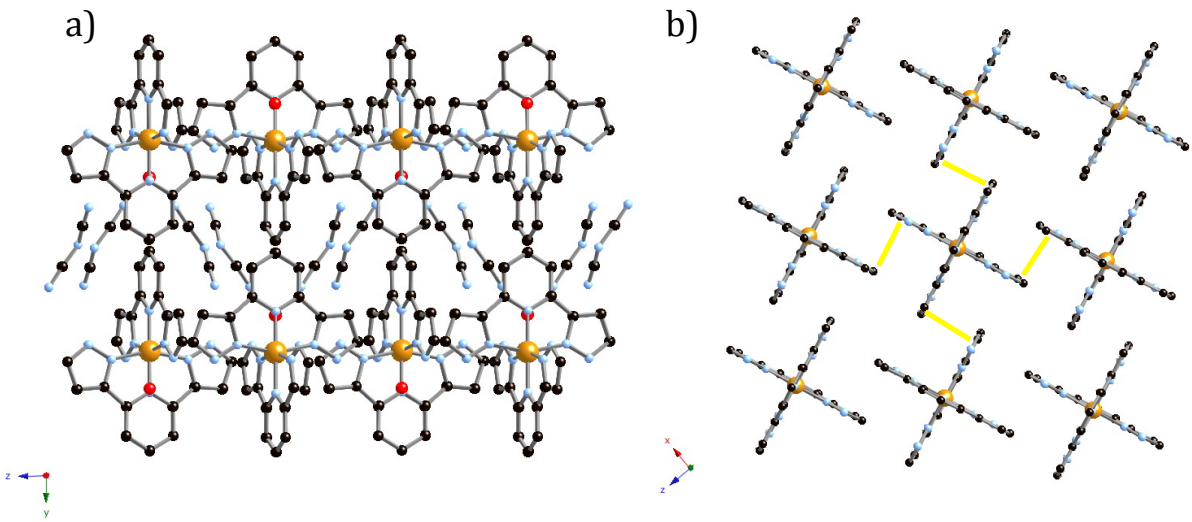

Figure S2: (a) A projection of the crystal structure of **2** showing (a) alternating cationic and anionic layers onto the *zy* plane and (b) the arrangement of $[Fe(bpp)_2]^{2+}$ units onto the *xz* plane (yellow lines refer to π– π interactions). H atoms are omitted for clarity. Color code for the atoms as it is indicated as follow: carbon, nitrogen, oxygen and hydrogen atoms are shown as black, blue, red and light-pink, respectively.

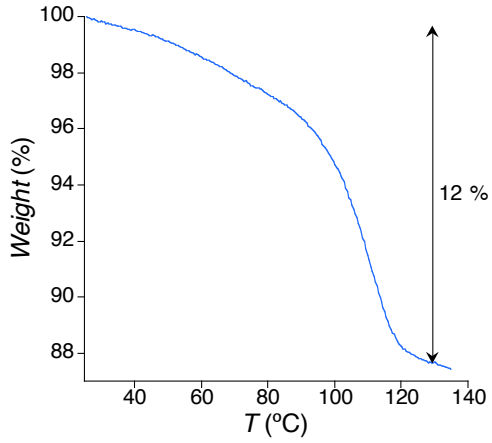

Figure S3: Weigh loss for the deshydration of **1**.

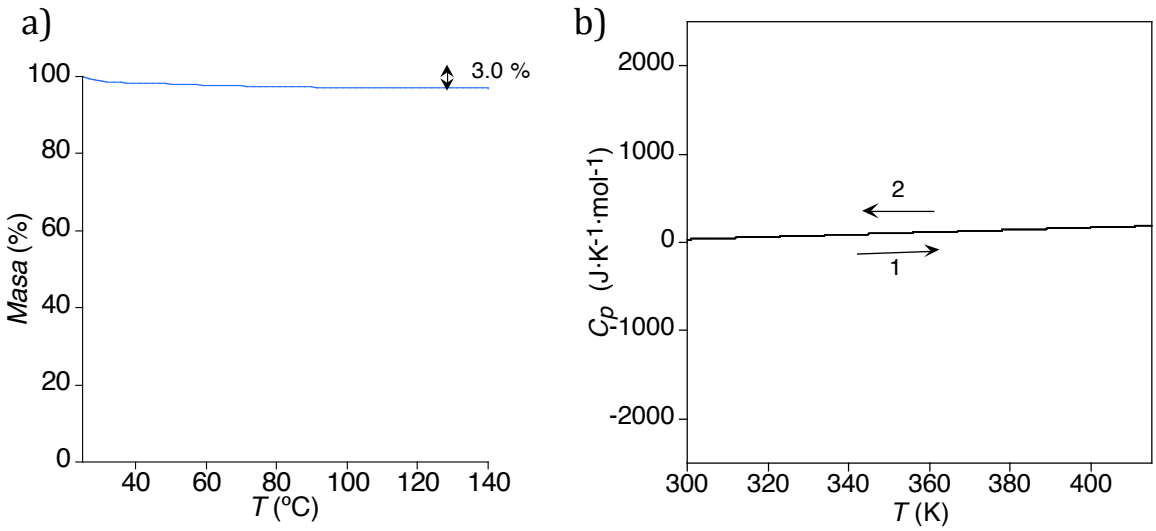

Figure S4: a) TGA and DSC (curve 1: original sample in the heating mode, curve 2: subsequent temperature cycle in the cooling mode) of compound **2**.

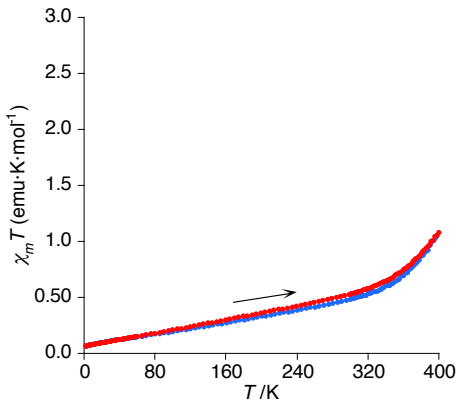

Figure S5: Temperature dependence of $\chi_m T$ in the temperature range between 2–400K on heating and cooling mode for **2** and the rehydrated sample (**2r**). Successive temperature cycles (on cooling and heating mode) have been omitted for simplicity, as they all go through the same place.

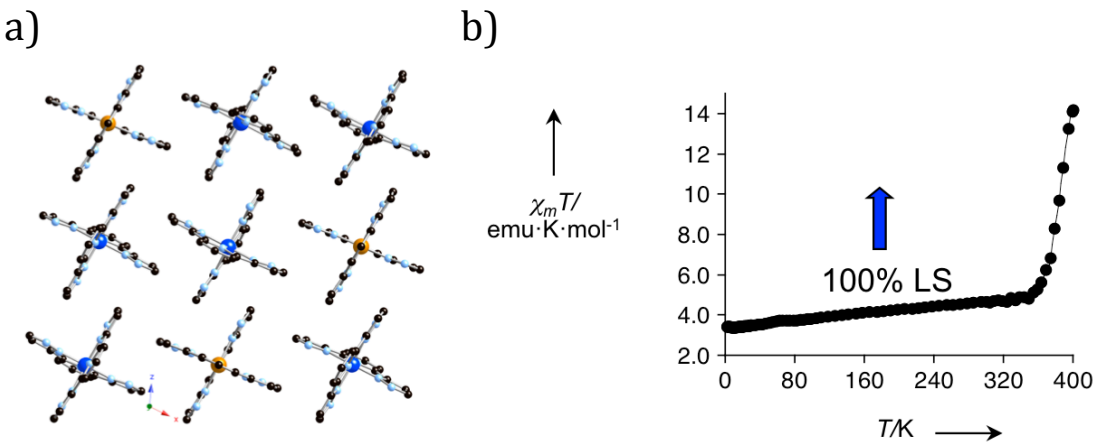

Figure S6: a) View of the $[Fe(bpp)_2]^{2+}$ layer in **1** down the *y* axis. Fe(1) is shown yellow and Fe(2) blue. Color code for the atoms as it is indicated in Figure **S2.** H atoms are omitted for clarity. B) Temperature dependence of $\chi_m T$ for compound **1** in the 2–400 K range.

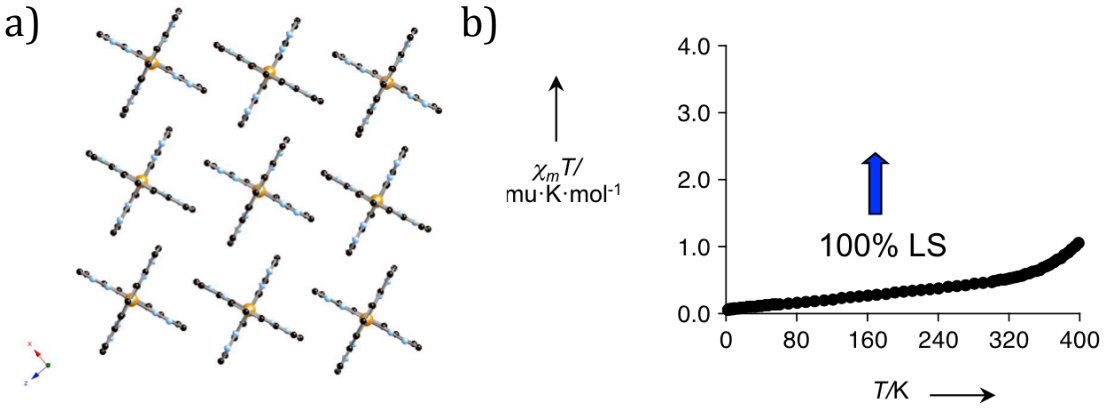

Figure S7: View of the $[Fe(bpp)_2]^{2+}$ layer in **2** down the *y* axis. H atoms are omitted for clarity. Color code for the atoms as it is indicated in Figure **S2.** B) Temperature dependence of $\chi_m T$ for compound **2** in the 2–400 K range.

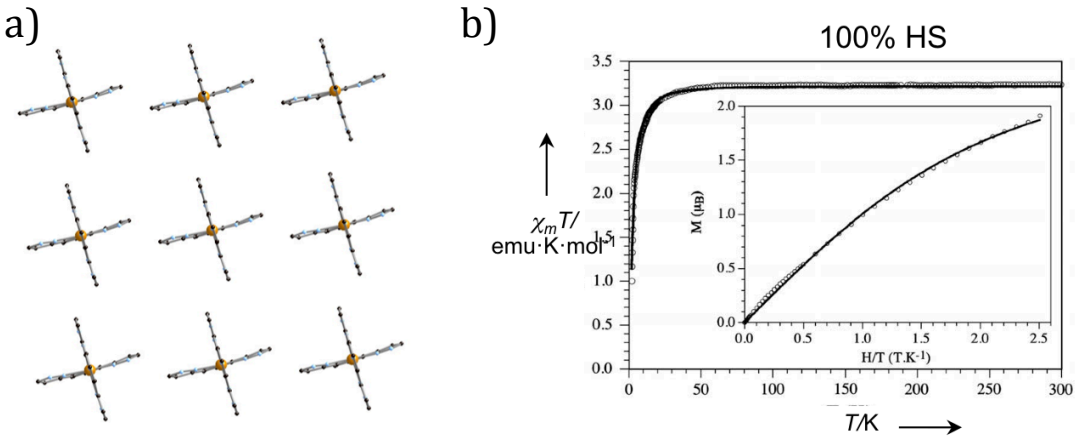

Figure S8: View of the $[Fe(bpp)_2]^{2+}$ layer in **4** down the *y* axis. H atoms are omitted for clarity. Color code for the atoms as it is indicated in Figure **S2**. B) Temperature dependence of $\chi_m T$ for compound **3** in the 2–400 K range.

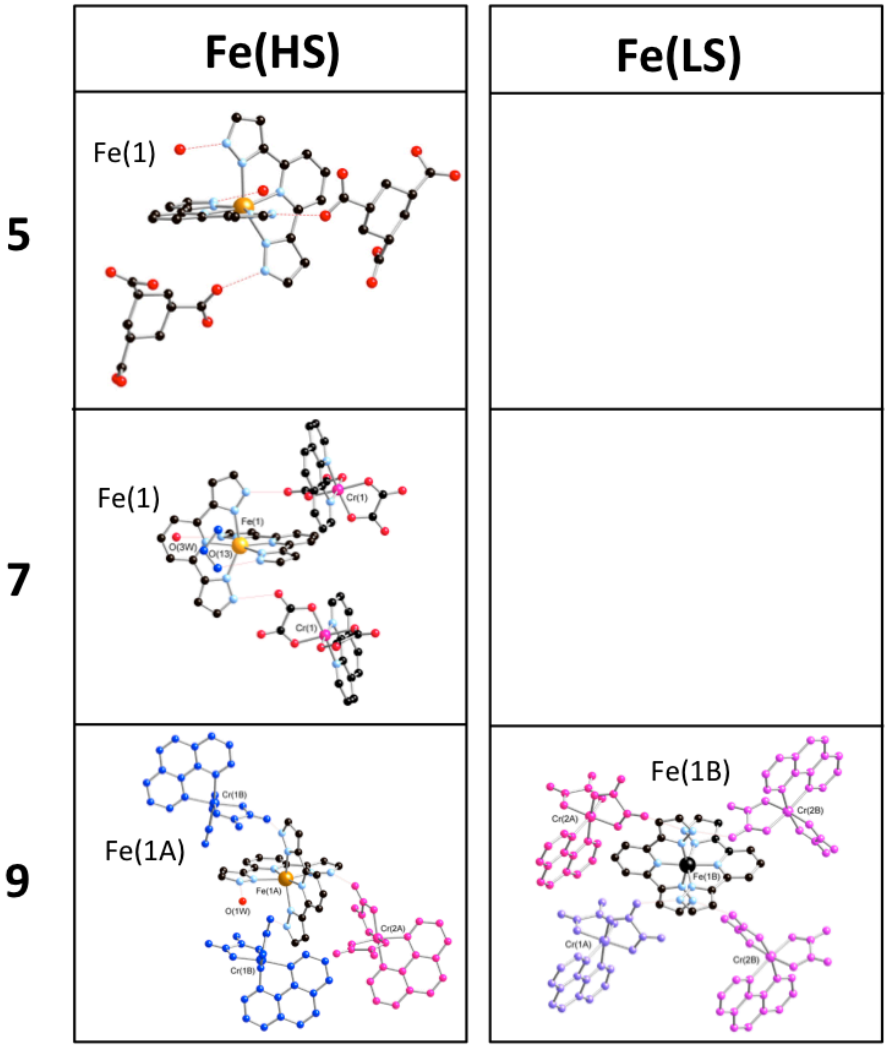

Figure S9: Composition of the second coordination sphere of the HS and LS Fe^{2+} centers for **5**, **7** and **9**. The same color has been used for all the atoms for the same crystallographic anion for the sake of clarity.

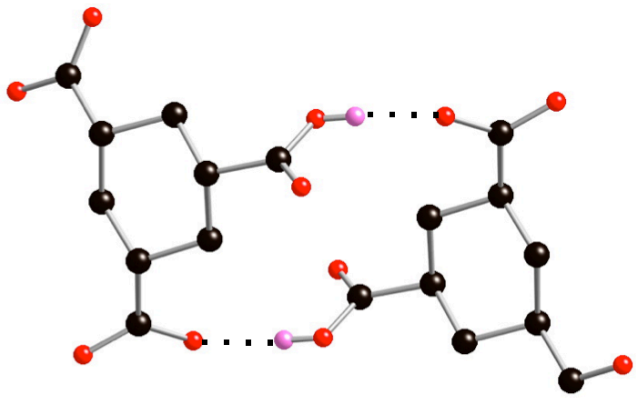

Figure S10: Supramolecular synthon ($[Hchtc]_2^{4-}$) found in the crystal structure of **5**. Carbon, oxygen and hydrogen atoms are shown as black, red and pink, respectively.

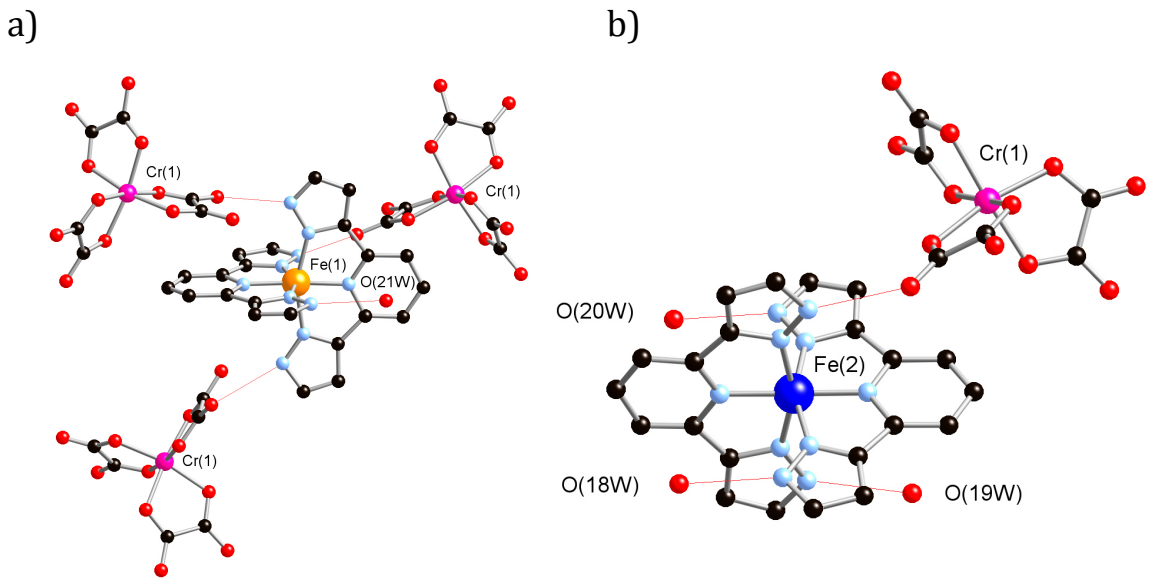

Figure S11: View of the crystal structure of the hydrated salt $[Fe(bpp)_2]_2[Cr(ox)_3]ClO_4{\cdot}5H_2O$ showing the first and second coordination spheres for the two crystallographic independent Fe^{2+} cations, Fe(1) (a) and Fe(2) (b). Carbon, oxygen and nitrogen atoms are shown as black, red and light-blue, respectively. H atoms are omitted for clarity.

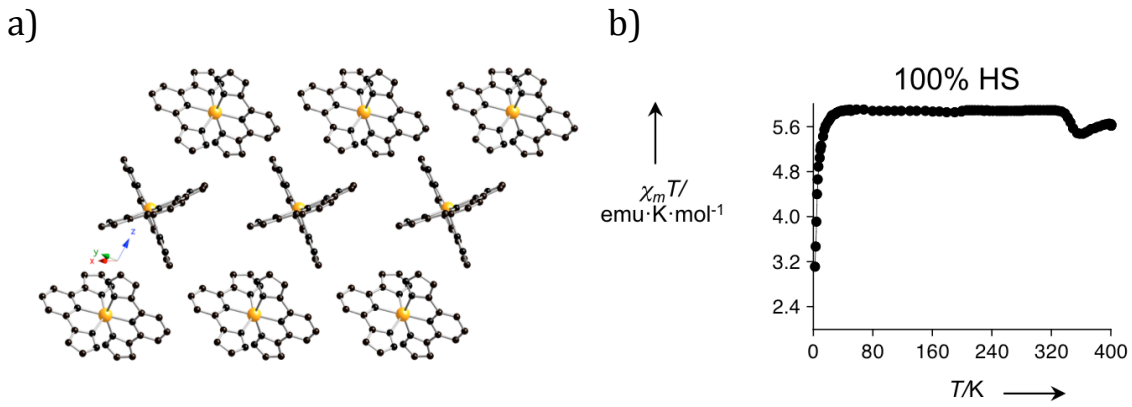

Figure S12: View of the $[Fe(bpp)_2]^{2+}$ layer in **7**. H atoms are omitted for clarity. B) Temperature dependence of $\chi_m T$ for compound **7** in the 2–400 K range.

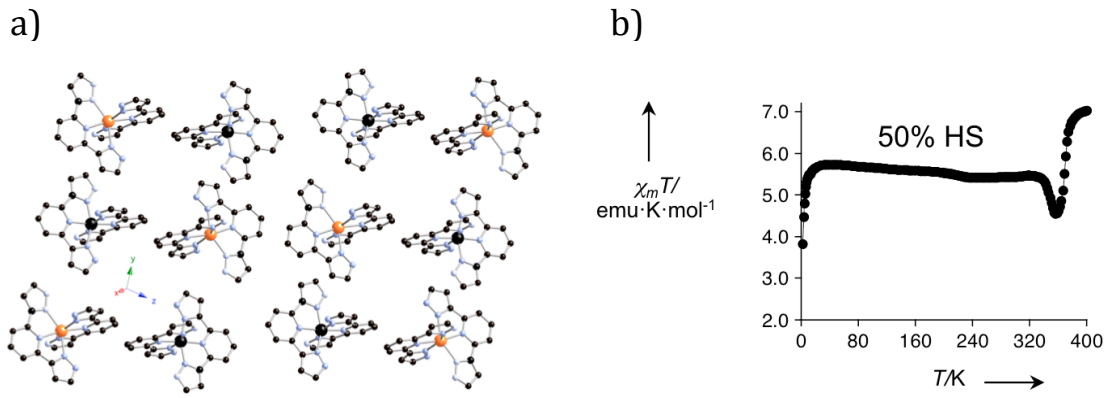

Figure S13: View of the $[Fe(bpp)_2]^{2+}$ layer in **8** down the *x* axis. H atoms are omitted for clarity. Color code for the atoms as it is indicated in Figure **S2**. B) Temperature dependence of $\chi_m T$ for compound **8** in the 2–400 K range.

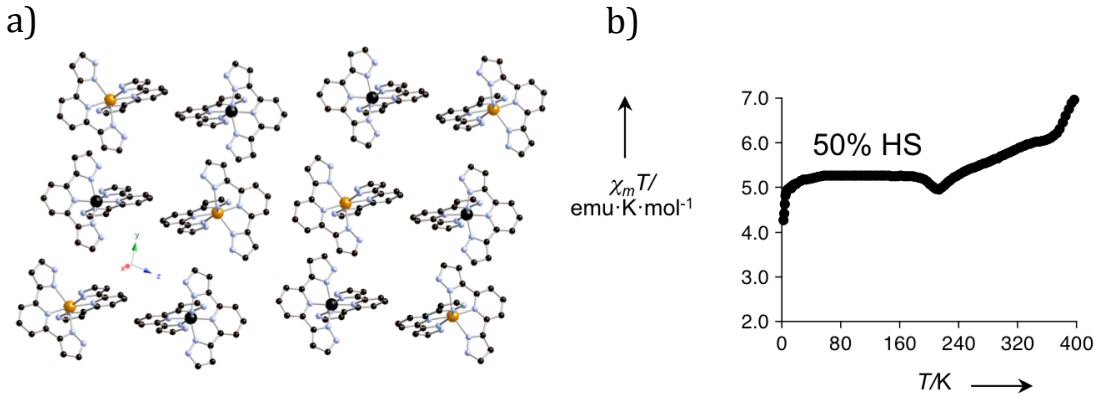

Figure S14: View of the $[Fe(bpp)_2]^{2+}$ layer in **9** down the *x* axis. H atoms are omitted for clarity. Color code for the atoms as it is indicated in Figure **S2**. B) Temperature dependence of $\chi_m T$ for compound **9** in the 2–400 K range.

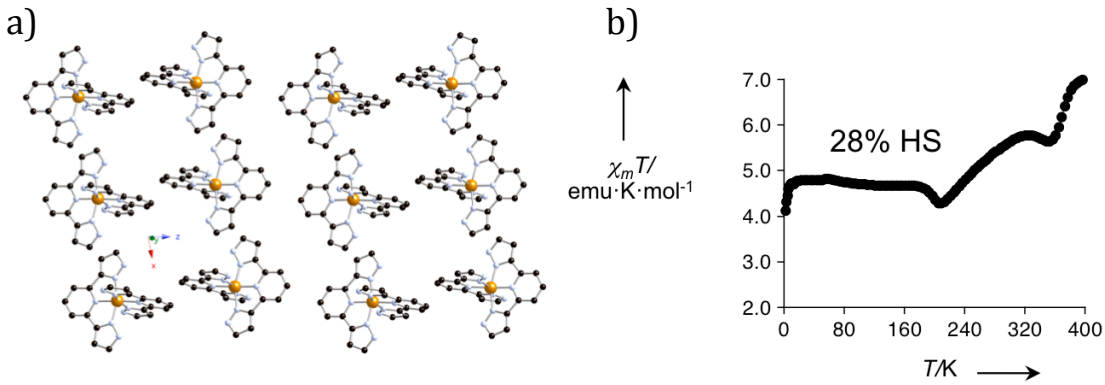

Figure S15: View of the $[Fe(bpp)_2]^{2+}$ layer in **9r** down the *x* axis. H atoms are omitted for clarity. Color code for the atoms as it is indicated in Figure **S4**. B) Temperature dependence of $\chi_m T$ for compound **9r** in the 2–400 K range.

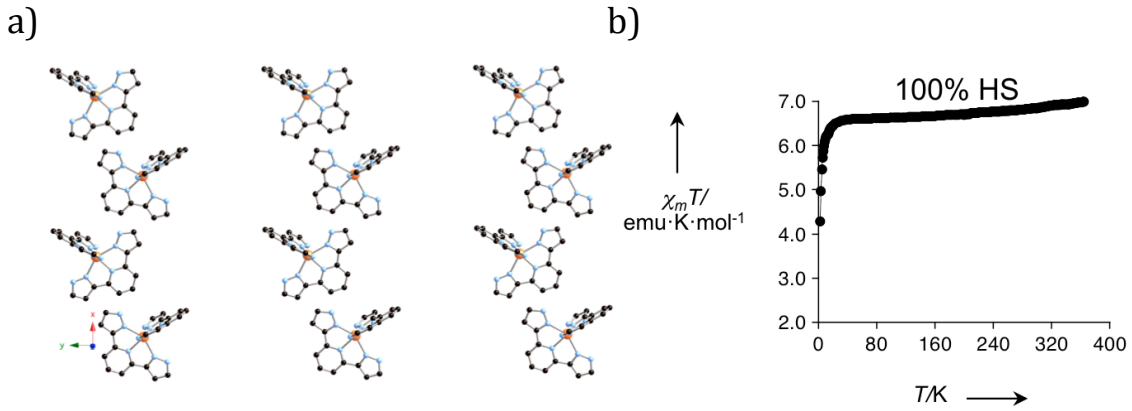

Figure S16: View of the $[Fe(bpp)_2]^{2+}$ layer in **10** onto the *xy* plane. H atoms are omitted for clarity. Color code for the atoms as it is indicated in Figure **S2**. B) Temperature dependence of $\chi_m T$ for compound **10** in the 2–400 K range.

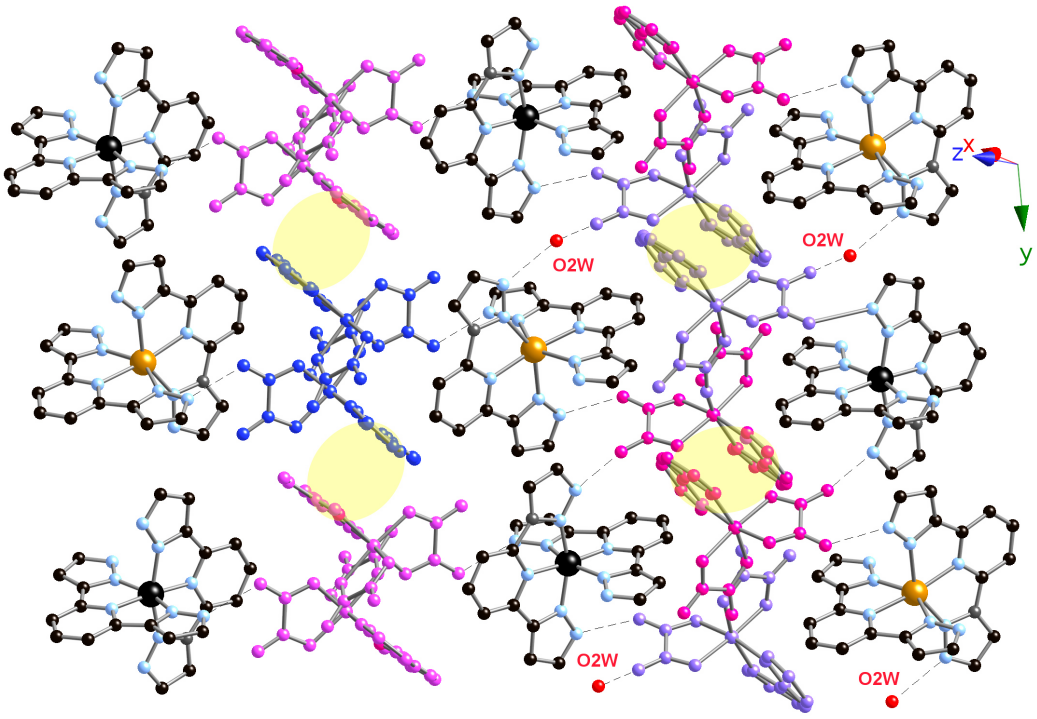

Figure S17: π-π stacking interactions between bpy ligands of neighboring $[Cr(bpy)(ox)_2]^-$ anions (3.583(2)–3.742(1) Å) for **8** are shown here in yellow.

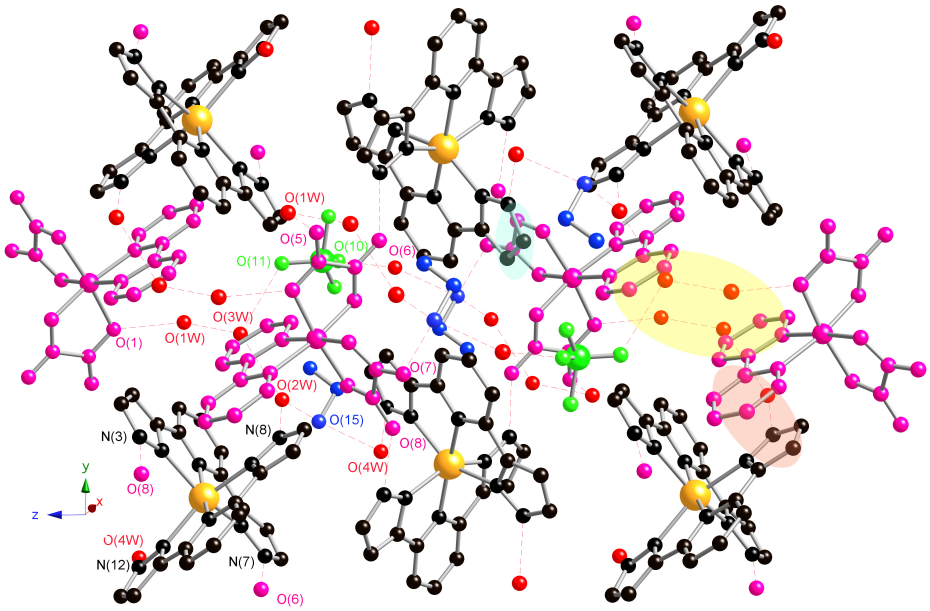

Figure S18: π-π stacking interactions between bpy ligands of neighboring $[Cr(bpy)(ox)_2]^-$ anions (3.270(4) Å) and between a bpy ligand and a bpp ligand (3.317(5)–3.341(5) Å) for **6** are shown here in yellow and light-orange, respectively.

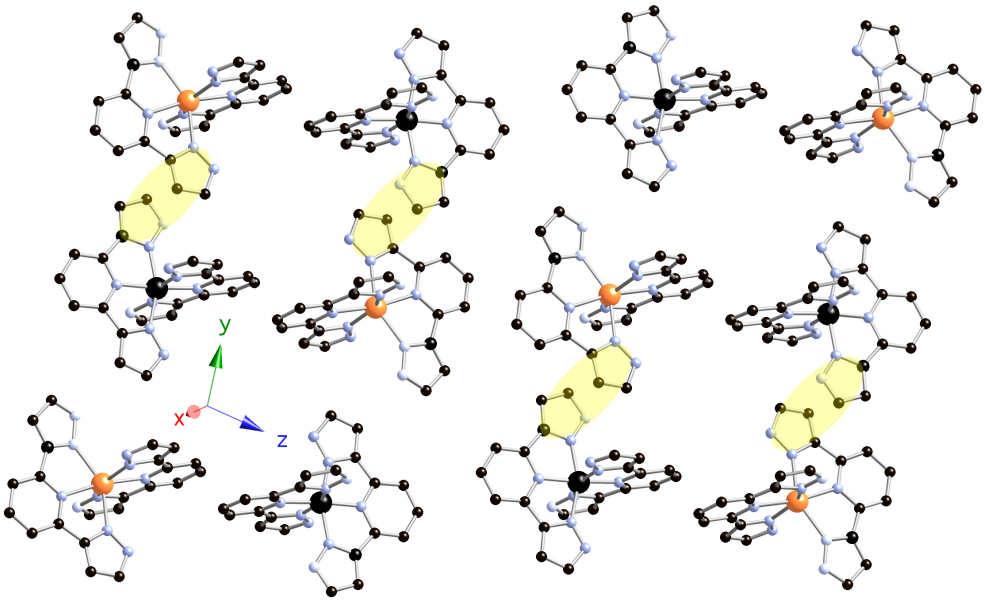

Figure S19: Aryl–aryl interactions between $[Fe(bpp)_2]^{2+}$ complexes (3.204(3) Å) within a 2D layer for **8** are shown here in yellow.